

X-ray beam hardening correction for measuring density in linear accelerator industrial computed tomography^{*}

ZHOU Ri-Feng(周日峰)¹⁾ WANG Jue(王珏) CHEN Wei-Min(陈伟民)

(Key Laboratory of Optoelectronic Technology and System of the Education Ministry of China,
ICT Research Center, Chongqing University, Chongqing 400044, China)

Abstract Due to X-ray attenuation being approximately proportional to material density, it is possible to measure the inner density through Industrial Computed Tomography (ICT) images accurately. In practice, however, a number of factors including the non-linear effects of beam hardening and diffuse scattered radiation complicate the quantitative measurement of density variations in materials. This paper is based on the linearization method of beam hardening correction, and uses polynomial fitting coefficient which is obtained by the curvature of iron polychromatic beam data to fit other materials. Through theoretical deduction, the paper proves that the density measure error is less than 2% if using pre-filters to make the spectrum of linear accelerator range mainly 0.3 MeV to 3 MeV. Experiment had been set up at an ICT system with a 9 MeV electron linear accelerator. The result is satisfactory. This technique makes the beam hardening correction easy and simple, and it is valuable for measuring the ICT density and making use of the CT images to recognize materials.

Key words linac ICT, beam hardening correction, density measurement

PACS 81.70.Tx

1 Introduction

ICT is a non-contacting and non-destructive inspection technique which provides cross-sectional images that allow the detection, location, and sizing of defects. It also provides information on the local material X-ray attenuation coefficients at each point in the image. In terms of the Beer's law, the attenuation of the monochromatic X-ray beam ($\ln(I_0/I)$) is linearly dependent on the mass density when passing through the same thickness. ICT makes use of this information and reconstructs an ICT image to find the composition of the objects and the density difference in the form of grayscale^[1]. However, the beam used with wide energy spectrum in the ICT, also called the polychromatic beam, is composed of different energy photons. When photons pass through the object, the lower energy photons are more strongly absorbed than the higher ones. Therefore, the energy spectrum of the beam changes, the average energy of photons

is improved and the beam seems to become "harder", which is called beam hardening. Because of this, the attenuation of a homogeneous object is not proportional to the density of the object. It also brings cup, streaks, and pronounced edges artifacts for ICT images^[2-5]. Fig. 1 is the attenuation profiles through a homogeneous iron cylinder of 150 mm in diameter. As seen from the grayscale curve in the figure, the cup artifacts are severe. It is obvious that there is an over 10% difference between the density measure value in the edge and that in the middle if the density measurements of the ICT image are directly done.

At present, there are a lot of methods about beam hardening. To give a short review on beam hardening corrections, the most common methods are presented subsequently. One of the first approaches to reduce the effects of the beam hardening is hardware filters. These filters which are made of diverse materials like aluminum, copper or brass are used to harden the X-ray. However, if the filter is too thick, it will absorb

Received 3 June 2008

^{*} Supported by National Natural Science Foundation of China (60672098)

1) E-mail: zurifg@163.com

©2009 Chinese Physical Society and the Institute of High Energy Physics of the Chinese Academy of Sciences and the Institute of Modern Physics of the Chinese Academy of Sciences and IOP Publishing Ltd

superfluous photons that make the total amount of X-ray reduce too much, and consequently, debase the signal-to-noise ratio of the detector system. On the other hand, the filter being too thin, the hardening artifacts are not completely eliminated^[6].

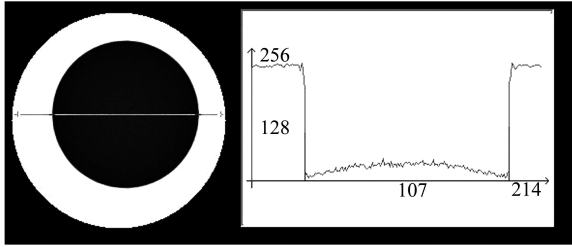


Fig. 1. The grayscale curve of ICT image of an iron cylinder.

The second correction method is named the dual energy method^[1, 2]. It utilizes two characteristic spectrum peaks of the K and L shells of the anode material of the source to perform the hardening correction. This method has many merits at low energy. But the two feature spectrum peaks are not obvious in the bremsstrahlung spectrum of X-ray which is produced by a high energy accelerator. Therefore, this correction method cannot suit ICT with a high energy linear accelerator.

The commonest correction method is the linearization technique^[3, 7, 8]. Virtually, by this method we can obtain relative curve between the attenuation of the polychromatic beam ($\ln(I_0/I)$) and the thickness of the object by experiments, and then perform a polynomial regression to make it equivalent to a linear curve between the attenuation of monochromatic beam and the thickness of the object. However, the drawback with linearization is that it requires calibration measurements of polychromatic reprojection for different thicknesses of the object material. This can be laborious, especially if many different materials are to be inspected as in most industrial applications. Another drawback is that it assumes homogeneous materials. However, for industrial application the objects often are not homogeneous and a priori knowledge of the material composition and density generally are unobtainable.

Fortunately, if the photon energy is between 0.3 MeV and 3 MeV, the diversity of the mass attenuation coefficient $\mu_m(E)$ in average metal is less than 2%. In the second section of this paper we have proved that the effect of the diversity of the mass attenuation coefficient is limited. The correction method which is presented in the second section associates hardware filtration with equivalent monochromatic method to obtain the attenuation curves, and

regresses equivalent monochromatic data to reconstruct CT image. This method conquers the disadvantages of the two methods mentioned above and makes this correction method suitable for the homogeneous material as well as different density materials (steel, aluminum, copper, titanium alloy, etc).

2 Theory and method

While propagating through the specimens which are made of i sorts of material, polychromatic X-rays with an incoming intensity I_0 are attenuated according to the material characteristics. These characteristics are expressed by the linear attenuation coefficient $\mu_i(E)$. This physical effect of attenuation is described by the Beer's law:

$$p(r) = -\ln \frac{I(r)}{I_0} = -\ln \left(\int S(E) e^{-\sum_{i=1}^n \mu_i(E) \cdot l_i(r)} \lambda(E) dE \right), \quad (1)$$

where $\lambda(E)$ is the detector efficiency; $l_i(r)$ is the project distance in the i material along r ; and $S(E)$ is the energy spectrum of X-rays, which meets $S(E) > 0$, $\int S(E) dE = 1$, additional

$$\mu_i(E) = \mu_{im}(E) \cdot \rho_i, \quad (2)$$

where $\mu_{im}(E)$ is the mass attenuation coefficient of the i substance, and its density is ρ_i .

As can be seen from Table 1, in the energy range of 0.3—3 MeV, the value of $\mu_{im}(E)$ of a different substance is approximately the same, particularly for Fe and Cu, the relative error is even less than 1%.

Table 1. Attenuation coefficients of Cu, Fe, Zn, Ti, and Al under various photon energy.

photon/MeV	Cu(29)	Fe(26)	Zn(30)	Ti(22)	Al(13)
0.3	0.1119	0.1062	0.1041	0.1043	0.1042
0.6	0.0762	0.0770	0.0769	0.0753	0.0780
1.0	0.0590	0.0599	0.0594	0.0589	0.0614
1.2	0.0537	0.0546	0.0540	0.0537	0.0561
1.5	0.0480	0.0488	0.0484	0.0480	0.0500
2.0	0.0420	0.0426	0.0424	0.0418	0.0432
2.5	0.0384	0.0387	0.0387	0.0381	0.0387
3.0	0.0360	0.0360	0.0363	0.0351	0.0354

So let

$$\mu_{im}(E) = K(E). \quad (3)$$

Using Expression (1)—(3), we can obtain Eq. (4)

$$p(r) = -\ln \left(\int S(E) e^{-K(E) \sum_{i=1}^n \rho_i \cdot l_i(r)} \lambda(E) dE \right), \quad (4)$$

For the monochromatic beam, by the Beer's law, we can acquire

$$m(r) = -\ln \frac{I(r)}{I_0} = -K(E_0)\lambda(E_0) \sum_{i=1}^n \rho_i \cdot l_i. \quad (5)$$

Using Eqs. (4), (5), we acquire Eq. (6)

$$p(r) = -\ln \left(\int S(E) e^{-K(E) \cdot m(r) / K(E_0)\lambda(E_0)} \lambda(E) dE \right). \quad (6)$$

Eq. (6) implies $p(r)$ is a function of $m(r)$ and $S(E)$, which is independent of the substance i . The answer of $m(r)$ in Eq. (6) can use polynomial regression^[9]. So, the acquired polynomial coefficient is suitable for all substances.

As we all know, the spectrum of linear accelerator is polyenergetic, and the low energy photon is in the majority. To absorb the low energy photons, pre-filters of the spectra below 0.3 kV have to be used. The change of the spectrum shown in Fig. 2 indicates that we have got the beam source whose photon energy range of 0.3 MeV to 3 MeV is mainly from the 9 MeV linear accelerator.

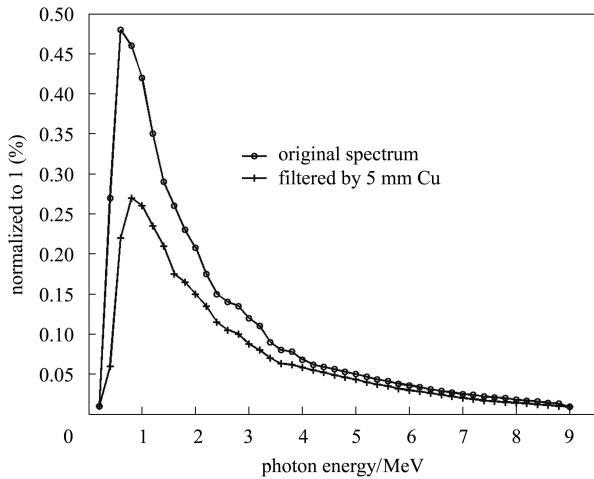


Fig. 2. The change of the spectra of 9MeV linac after filters (simulated by EGSnrc program).

Experiments are conducted to show the nonlinear relation between the iron thickness d and the attenuation when the photon energy ranges between 0.3 MeV to 3 MeV. The beam hardening effect is shown in Fig. 3. The curve is the iron attenuation of the polychromatic beam, and via regression to attenuation of the monochromatic beam to correct the ICT data^[10]. This correction cure can be used to correct the artifacts of object made of average metals also, and the measure error is less than 2% theoretically.

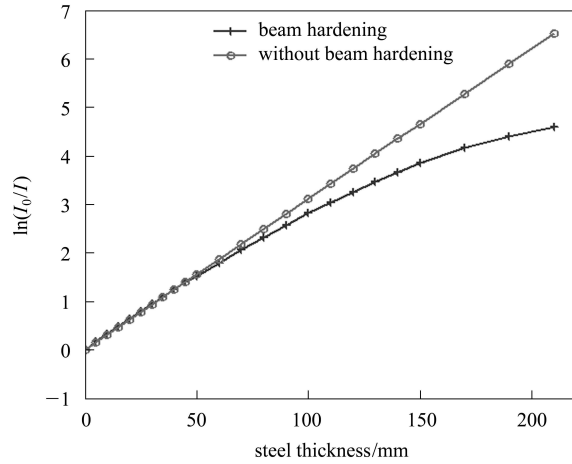


Fig. 3. The beam hardening effect causes a nonlinear relation between the iron thickness d and the attenuation.

3 Measurements and results

The experiment which was conducted to examine the validity of the method was carried out in an ICT with a 9 MeV electron linear accelerator, and the pre-filters were used. An iron cylinder with 150 mm in diameter was taken as the test object. The results are shown in Fig. 4. The upper part of the figure is the image before using beam hardening correction, while its lower part is the beam hardening correction result. The image quality reveals that this beam hardening correction algorithm can substantially reduce the cupping distortion.

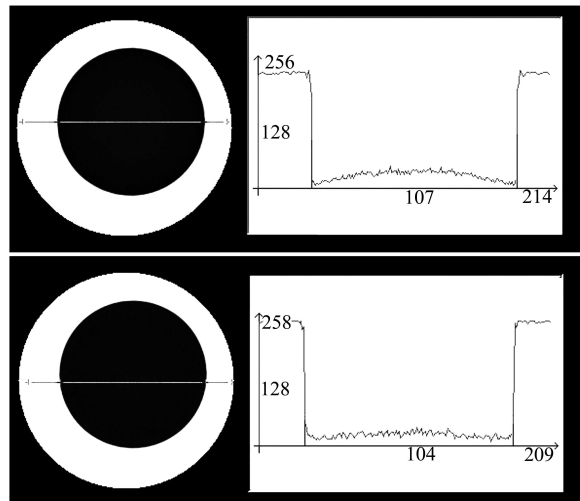


Fig. 4. Reconstructive graph of iron tray with beam hardening correction or not (the upper is before beam hardening correction and the lower is after).

The density test model is composed of seven cylinders of 30 mm each in diameter. The cylinders are

materials of copper, steel, titanium, aluminum alloy, tetrafluoroethylene, plastic and methacrylate. Fig. 5 is the CT image of the test model after using linearization beam hardening correction. The density measurement result and measurement precision are shown in Table 2. It shows that the relative error is even less than 1.68% even when many different materials are to be inspected at a time.

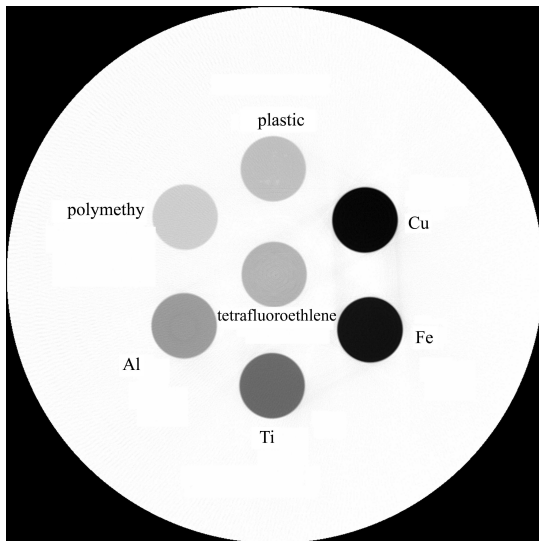


Fig. 5. CT image of the objects consists of seven different materials.

Table 2. Errors for density measurement of some different materials after beam hardening correction.

material	factual density /(g/cm ³)	CT measure density/(g/cm ³)	relative error δ (%)
copper	8.37	8.40	0.36
steel	7.85	7.845	0.06
titanium alloy	4.43	4.42	0.12
aluminum alloy	2.80	2.77	0.36
tetrafluoroethylene	2.16	2.03	1.55
plastic	1.59	1.61	1.25
polymethyl	1.19	1.21	1.68
methacrylate			

4 Conclusion

The advantages and disadvantages of popular beam hardening correction methods are discussed, and a suitable method is presented. This method, which associates hardware filtration with linearization equivalent monochromatic method, has been applied to the ICT device with a 9MeV accelerator, and the density measure error is less than 2% among seven kinds of materials. This result is in perfect accordance with the theory. It indicates that this technique is easy, simple, and avoids laborious work, and that it is valuable for measuring the ICT density and making use of the CT images to recognize materials. We hope that this correction will encourage more research on the beam hardening method and will lead to greatly improving the precision for measuring the ICT density.

References

- 1 van de Castele R, van Dyck D, Sijbers J et al. *Physics in Medicine and Biology*, 2002, **47**: 4181
- 2 Krumm M, Kasperl S, Franz M. *NDT&E International*, 2008, **41**: 242
- 3 Brooks R A, Chiro G Di. *Physics in Medicine and Biology*, 1976, **21**(3): 390
- 4 Duerinckx A J, Macovski A. *Journal of Computer Assisted Tomography*, 1978, **2**(4): 481
- 5 Rao P S, Alfidi R J. *Radiology*, October, 1981, **141**: 223
- 6 Zatz L M, Alvarez R E. *Radiology*, 1977, **124**: 91
- 7 Hammersberg P, Angard M. *Journal of X-ray Science and Technology*, 1998, **8**(1): 75
- 8 Herman G T. *Physics in Medicine and Biology*, 1979, **24**(1): 81
- 9 Herman G T. *The Fundamentals of Computerized Tomography*. New York: Academic Press, 1980. 23—30
- 10 ZENG Gang et al. *HEP&NP*, 2006, **30**:178 (in Chinese)